A Monte Carlo Simulation Platform for Studying Low Voltage Residential Networks

Ricardo Torquato, *Student Member, IEEE*, Qingxin Shi, *Student Member, IEEE*, Wilsun Xu, *Fellow, IEEE*, and Walmir Freitas, *Member, IEEE*

Abstract—The smart grid vision has resulted in many demand side innovations such as nonintrusive load monitoring techniques, residential micro-grids, and demand response programs. Many of these techniques need a detailed residential network model for their research, evaluation, and validation. In response to such a need, this paper presents a sequential Monte Carlo (SMC) simulation platform for modeling and simulating low voltage residential networks. This platform targets the simulation of the quasi-steady-state network condition over an extended period such as 24 h. It consists of two main components. The first is a multiphase network model with power flow, harmonic, and motor starting study capabilities. The second is a load/generation behavior model that establishes the operating characteristics of various loads and generators based on time-of-use probability curves. These two components are combined together through an SMC simulation scheme. Four case studies are presented to demonstrate the applications of the proposed platform.

Index Terms—Demand response, low voltage residential networks, microgrids, network simulation, power quality.

I. INTRODUCTION

LOW-VOLTAGE (LV) residential electric networks have become a frontier of smart grid research and development due to a number of demand side innovations. Examples are the roof-top photovoltaic (PV) panels, electric vehicles (EVs) and associated vehicle-to-grid operation, demand response programs, home energy use monitoring, and residential micro-grids, etc. [1]. Such developments have resulted in a great need for tools that can model and simulate residential networks properly and effectively. The tools are expected to support a number of demand side related smart grid research activities, as illustrated below.

1) *Nonintrusive Load Monitoring (NILM) Research:* This research attempts to determine the energy use of individual home appliances based on the power measured at the service entrance point only [2], [3]. Due to its significant energy-saving and data analytic potentials, NILM has become a very hot research topic pursued by various disciplines [3]–[6]. A notable challenge faced by this research is how to verify the numerous NILM algorithms published. A detailed simulation platform that can model the electrical behaviors of various home appliances is one of the attractive solutions to this challenge.

2) *Integration of Local Generators (such as PVs), New Loads (such as EVs), and Energy Storage Devices:* A number of research topics have been proposed in this direction, such as optimal operation of the residential network, switching between grid-connected and islanded modes, minimization of load-generation imbalance, etc. A proper simulation platform is an essential tool for evaluating the performance of various proposed or published techniques.

3) *Power Quality Concerns:* The adoption of new load and generation technologies in homes and LV networks has raised concerns on their potential power quality impacts. An example concern is the neutral-to-earth voltage (NEV) rise due to the connection of large loads such as EV chargers between phase and neutral [7], which could lead to stray voltage incidents. Another concern is the harmonic interactions among the devices. Detailed low-voltage network models are needed to analyze such problems.

4) *Demand Response Studies:* Demand response programs control the operation of certain appliances in homes or influence their operation through means such as time-of-use pricing. To predict the effectiveness of a demand response program, one has to understand, model, and simulate the household energy consumption characteristics [8], [9]. Since the home appliances operate in a probabilistic manner, a large number of Monte Carlo style simulations are needed to determine the outcome of demand response programs statistically.

In response to the above needs, this paper proposes a generic low voltage residential network simulation platform that can be used to evaluate many of the demand side smart grid ideas and techniques. The platform takes into account the common characteristics of the four research areas identified earlier. It covers an extended simulation period of at least 24 h and has an output resolution of one snapshot per second. The proposed concept, to some extent, is similar to that of power system dispatcher training simulators [10], but the modeling issues and target applications are completely different. The dispatcher training simulators simulate the steady-state

transmission network responses associated with contingencies, generation dispatches, operator actions, etc. They are designed for training transmission system operators, implemented using deterministic, single-phase load flow methods, and can accept operator intervention. The proposed simulator, on the other hand, is designed to simulate low voltage residential systems. The main characteristics of such systems are: 1) random load variations; 2) multiphase network topology; 3) harmonics and motor starting transients; and 4) no operator intervention. The applications of the simulator are to provide a platform and data for researching demand responses, NILM algorithms, the impact of new residential loads, and generators.

This paper is organized as follows. The main requirements on and the characteristics of the proposed simulation platform are explained in Section II. Section III presents methods to model the behavior of randomly operating loads and local generators. Section IV explains the techniques to model and solve the residential electric networks. Section V combines both behavior and electrical models to arrive at the overall simulation platform and its algorithm. Case study results are presented in Section VI to demonstrate the applications of the platform.

II. PROPOSED SIMULATION PLATFORM

Similar to high voltage power system simulation and analysis, the residential network studies require two broad types of tools. One is to simulate the dynamic or steady responses of a network corresponding to a single event such as a short-circuit fault or a load change. Several commercial tools are available to meet the dynamic simulation needs (such as PSCAD/EMTDC and MATLAB/Simulink) and the steady-state simulation needs (such as CYME, PSS/Adept, and DIgSILENT). The second type is to simulate the quasi-steady-state behavior of a network over an extended period such as several hours mimicking a sequence of events happening in the system. Power system dispatcher training simulator is an example of such a tool for high voltage systems. To our knowledge, such a tool has not been developed for low voltage residential networks. The objective of the proposed platform is to address this need. Since it covers an extended period, a number of unique issues must be addressed, such as when an appliance will be switched-on, how long it will remain in operation, what is the typical solar irradiance level at different snapshots, etc. These issues will be discussed in this section.

A. General Requirements on the Simulation Platform

Through analyzing the common characteristics of the four research areas explained in Section I, the following general requirements have been identified for the quasi-steady-state simulation platform.

1) Extended Simulation Period: The operation of residential loads is highly time-dependent. For example, laundry activities are more likely to take place in the morning, while TVs are mostly switched-on in the evening. Many of the researches cited in Section I require modeling the network activities over at least a 24 h period, as the performance of various demand side techniques must be verified over an extended period. A NILM algorithm, for example, is expected to be able to identify the actions of major home appliances at any time of a day.

2) Modeling of Random Behaviors of Residential Loads and Generators: Since the loads and generators in the LV network operate in a random manner over the simulation period, the proposed tool must be able to handle probabilistic events. At any instant, the tool shall determine the operating status of a load or generator based on their operation profiles that are characterized with probabilistic distribution functions.

3) High Resolution Output: The platform should also be able to output the network responses at a resolution of one snapshot per second. This requirement is mainly due to the first application, i.e., to support the NILM researches. This is because NILM algorithms need to use as many electrical signatures of home appliances as possible. The proposed resolution is barely adequate to capture the motor starting transients which are significant signature for NILM algorithms.

4) Multiphase Network Model: The residential network is a multiconductor circuit with both phase-to-neutral and phase-to-phase connected loads. In addition, it has various grounding points whose grounding resistances can have an impact on the network responses. Therefore, the simulator must include every conductor of the system so that situations such as load imbalance, poor neutrals, and harmonic cancellations can be studied.

5) Harmonics and Motor Starting: Harmonics and motor starting transients produced by many residential loads carry unique electrical signatures. These signatures are used for appliance identification by many NILM algorithms. It is, therefore, very important for the simulation platform to model such signatures. Additionally, harmonics and motor starting transients are disturbances that must be assessed from power quality perspective.

The above requirements can be addressed by using two models for the LV network. One is the electrical model which represents the electrical characteristics of the network and loads. Another is the behavior model which covers the random operations of loads caused by the behavior of home inhabitants.

B. Electrical Model

This model represents the electrical characteristics of the simulated LV system, such as the network topology and impedances. A typical multiphase LV network of North America, selected for the proposed platform, is shown in Fig. 1. It contains a primary network equivalent (14.4 kV), a service transformer (14.4/0.12/0.24 kV), and several houses connected in parallel. Although the platform has been designed to cover any number of houses, ten is typically used on the studies. Each house is represented by a further detailed circuit comprising individual devices connected in different rooms (Fig. 2).

Note that the equivalent circuit for the primary network is a two-phase coupled Thévenin circuit. One phase (p) represents the energized conductor and the other phase (n) represents the neutral conductor. V_n models the neutral voltage rise caused
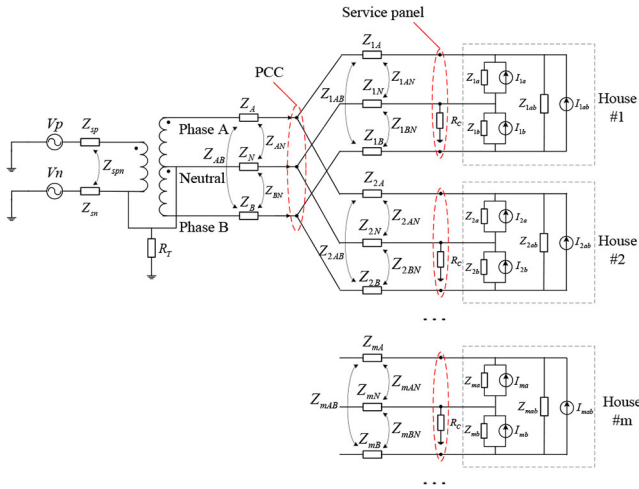
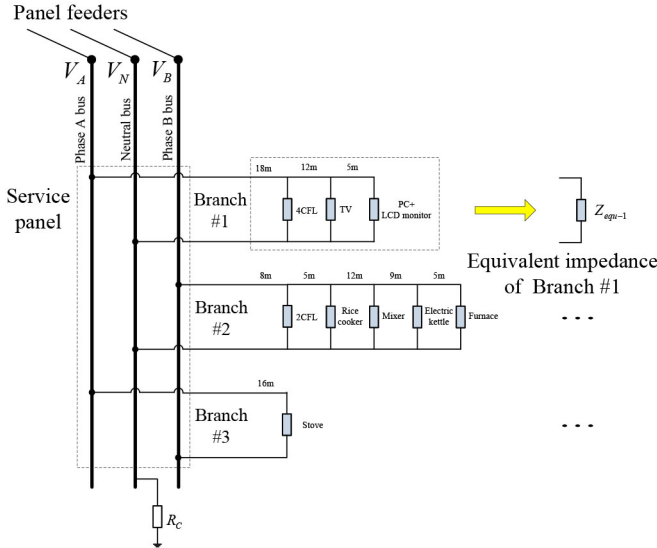Fig. 1. Generic multiphase low-voltage distribution network.

Fig. 2. Single-house detailed circuit.

by the upstream system and loads. This model is very general so one can use it to study the impact of primary system on the LV network.

C. Behavior Model

Behavior model here refers to the chronological operating characteristics of various loads or generators. For example, the behavior model of a microwave oven can be characterized using its on-instant, power setting, and off-instant. The behavior model of the simulator is responsible to determine the probabilistic load demand during the simulation. In other words, it establishes which devices are connected to the network at a particular instant based on the time-of-use probability characteristics of the device. An example output of the behavior model over a 24 h period is shown in Fig. 3. This figure shows the operating status of several common appliances (high value means in operation and low value means off-line).
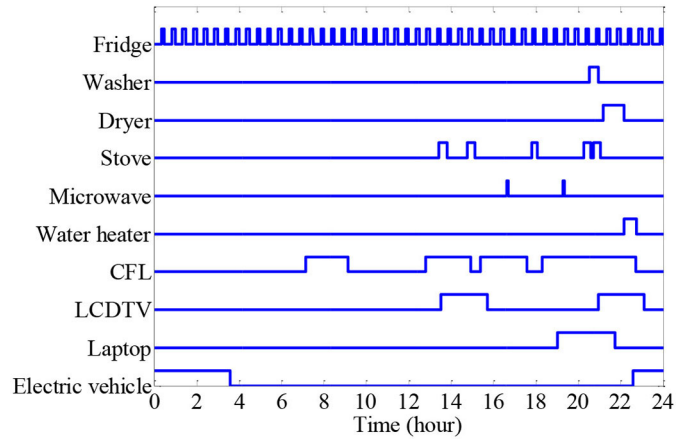

Fig. 3. Sample household load behavior profile.

D. Sequential Monte Carlo Simulation

The probabilistic operating characteristics of LV loads and generators make it impossible to predict the response of a residential network using a deterministic approach. A sequential Monte Carlo (SMC) simulation technique is adopted to address the problem. SMC is a computer simulation method based on probabilistic theory and statistical techniques. The main idea is to determine, at a given time t, the expected value of a function $F(X_{0:t})$, where $X_{0:t}$ represent the system states from time 0 to t. It may be determined using (1), where $p(X_i)$ is the probability of occurrence of state X_i. [11], [12]

$$E(F) = \sum_{i=0}^{t} F(X_i) p(X_i).\qquad(1)$$

When applied to this paper, the SMC simulation method will determine whether the expected operation status of an appliance at a given instant (or snapshot) is ON or OFF. Such status depends on the previous appliance states (if appliance was ON or OFF on previous instants). Therefore, SMC is applied to create a plausible residential behavior profile such as the one presented in Fig. 3, considering the time-of-use probability of the various devices connected to the network. Once such a behavior profile is created, it is combined with the network electrical model to create an instance of the network for that profile. This instance is a deterministic network. Multiphase power flow, harmonic power flow, and motor starting studies are then performed for the instance in a second-by-second sequence. This will yield the network responses over the simulation period for that instance.

In reality, there are many instances of load profiles. So the simulation is repeated many times for various randomly generated instances. Statistical analysis is then conducted on the results to obtain statistically valid performance indices.

III. BEHAVIOR SOLUTION METHOD

This section will present methods to determine the random operating states of residential loads and generators for a 24 h simulation period.
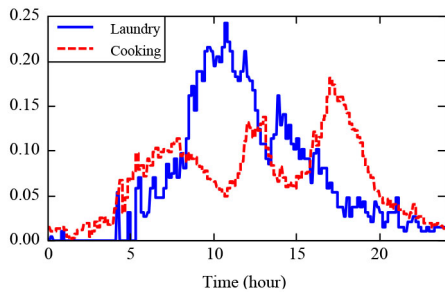
Fig. 4. Example of time-of-use probability profile for household activities.

Fig. 5. Charging profile for three EVs using different charging strategies.

A. Home Appliance Time-of-Use Probabilistic Behavior

To model a residential demand scenario, the simulator must determine a time distribution of the ON/OFF states for all home appliances. These are considered random events, since they directly depend on the behavior of residence occupants. Such behavior follows certain statistical distributions, usually referred to as the time-of-use probability curves [13], [14]. These curves represent the likelihood of a residence starting an activity at each instant of a day. They are obtained through load survey research and are expected to become more accurate and more detailed in the future with the support of increased data analytics capability of the smart grid. Example curves of laundry and cooking activities with data collected by load surveys [13], [14] are shown in Fig. 4.

These activities are associated with specific appliances, for example: washing machine and dryer are related to the laundry activity, while microwave and stove are related to cooking. Thus, using activity time-of-use profile, switch-on probability curves may be assigned to all home appliances. These curves represent the activities of a single day to be simulated. If an appliance is not active for that day (such as if laundry activity is not performed), the input data to the simulator can be changed by not including that appliance.

Such appliance behavior model is included into the simulator as follows: for each snapshot, if a certain appliance is OFF, a random number (r) uniformly distributed between 0 and 1 is generated. If r is smaller than the switch-on probability, the appliance is switched-on and remains ON for its associated working cycle duration, which is also randomly determined based on typical data for each appliance. Otherwise, it remains OFF. This procedure is repeated for every appliance, during the entire simulation period. The result is a time-of-use profile, such as that shown in Fig. 3.

B. EV Charging Behavior

The EV charging behavior is modeled by two random variables: 1) charging start time; and 2) charging duration. To some extent, EV behavior model is similar to appliance time-of-use probability curves; however, the modeling issues are distinct as described below.

EV charging start time is usually at night, when EV owners are at home, and during off-peak demand to take advantage of time-dependent tariffs. It is modeled by a normal probability density function (PDF) as in (2), where x is the plug-in
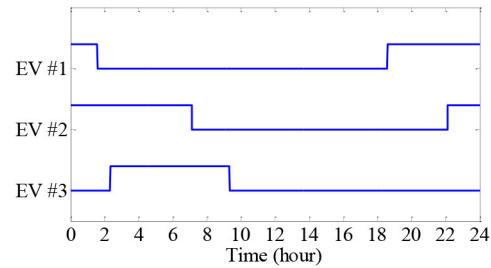
time; μ and σ are the average and standard deviation of x, respectively [15]. All variables are given in hours

$$f(x) = \frac{1}{\sigma\sqrt{2\pi}} e^{\left(-\frac{1}{2}\left(\frac{x-\mu}{\sigma}\right)^2\right)}, \qquad \mu = 1, \sigma = 3. \quad (2)$$

The charging duration time is determined according to the battery state of charge (SoC) when it is plugged-in. SoC is calculated by (3), where R is the maximum miles an EV can run from electric battery only; m is the number of miles traveled during 1 day, which is modeled by a lognormal PDF [16]

$$\text{SoC} = \begin{cases} \dfrac{R - m}{R} \times 100\% & 0 \leq m \leq R \\ 0 & m > R. \end{cases} \quad (3)$$

Once the battery SoC is determined, its charging time duration can be directly calculated according to the total battery capacity and the charger power level.

After determining charging start time and charging duration time variables, the EV behavior may be integrated into the LV simulation platform. Fig. 5 presents three charging examples.

C. Solar Irradiance Level Behavior

The power generated by a PV array is directly dependent on the incident solar irradiance level, which, in turn, depends on clouds intermittent behavior [17].

The Beta PDF is generally employed to model the solar irradiance variability for a single snapshot [18]. Although such approach has been used in a number of published works, it considers each snapshot is independent from each other. However, if a cloud starts covering the sun at 14:00, it is unlikely to disappear at 14:01. In view of this drawback, a new approach is herein proposed, based on historical measurements. The method will be introduced using actual historical data from Edmonton, Canada, although its parameters may be readjusted according to weather information available at the location under study.

The sky condition over one day is divided into four categories, according to the cloud coverage level (CCL): 1) clear; 2) partly clear; 3) mostly cloudy; and 4) overcast. CCL is quantified according to the solar irradiance level reaching the surface of earth (*Irr*); and its maximum value on a determined place (*Irr*$_{\max}$), both given in W/m^2, as in (4). For the city of Edmonton, CCL probabilities are presented in Table I [19], and a maximum irradiance level curve is extracted from historical measured data [23]. With such information, once a day-type

TABLE I
CLOUD COVERAGE LEVEL PROBABILITY FOR DIFFERENT
DAY-TYPES—EDMONTON, CANADA

Day-type	Cloud-type	Cloud coverage level	Probability of occurrence (%)
Clear	1	0.00-0.05	67.4
	2	0.05-0.15	18.6
	3	0.15-0.25	14.0
Mostly clear	4	0.25-0.35	38.5
	5	0.35-0.45	38.5
	6	0.45-0.55	23.0
Mostly cloudy	7	0.55-0.65	35.3
	8	0.65-0.75	41.2
	9	0.75-0.85	23.5
Overcast	10	0.85-0.95	45.0
	11	0.95-1.00	55.0

Fig. 6. Solar irradiance level prediction for a clear day.

is chosen, the daily solar irradiance curve may be forecasted according to the following algorithm:

$$\text{CCL} = 1 - \frac{Irr}{Irr_{\max}}. \tag{4}$$

Initially, a cloud-type (CT) is randomly chosen according to the probability of occurrence presented in Table I, for the correspondent day-type. According to the selected CT, CCL is randomly determined using (5), where Unif represents a uniform pdf, while $CCL_{\min}$ and $CCL_{\max}$ are, respectively, the minimum and maximum CCL for the correspondent CT presented in Table I

$$\text{CCL} = \text{Unif} \left([CCL_{\min}, CCL_{\max}]\right). \tag{5}$$

Since cloud forecast may be up to 80% inaccurate [24], cloud duration period may be randomly determined between 0 and 86 400 s (24 h). Therefore, cloud end time is given by (6), where t is the current simulation time snapshot (in seconds)

$$\text{endtime} = t + \text{Unif} \left([0, \ 86400]\right). \tag{6}$$

For each snapshot, a random correction factor is applied to CCL in order to model CCL variability within different snapshots. The corrected CCL value ($CCL_{\text{corrected}}$) is modeled by a normal distribution ($\text{Norm}(\mu, \sigma)$) with average (μ) equal to CCL and standard deviation (σ) of 0.05 as in (7). Negative values of $CCL_{\text{corrected}}$ are adjusted to zero

$$\text{CCL}_{\text{corrected}} (t) = \text{Norm} \left(\mu = \text{CCL}, \sigma = 0.05\right). \tag{7}$$

$CCL_{\text{corrected}} (t)$ is, then, applied to determine the current solar irradiance level using (8), where $Irr_{\max} (t)$ is the maximum irradiance for the corresponding instant t, and is given in W/m^2

$$Irr (t) = Irr_{\max} (t) \times [1 - \text{CCL}_{\text{corrected}} (t)]. \tag{8}$$

Equations (7) and (8) are repeated for the subsequent snapshots, until CT end time is reached. Once cloud duration has been completed, a new CT is randomly chosen and the algorithm must be repeated using (5)–(8).

By the end of the 24-h simulation, the solar irradiance level curve is determined. Fig. 6 presents a sample curve derived from the proposed algorithm, for a clear day. The irradiance
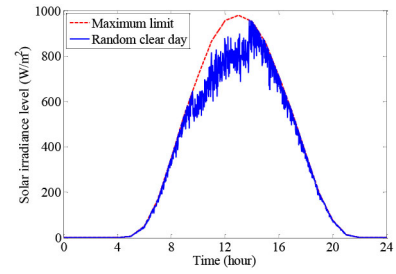
level is, indeed, close to the maximum ever recorded until 9:00, when a group of clouds cover part of incident irradiance. This behavior persists up to 14:00, when clouds disappear and the incident irradiance level becomes closer to its maximum limit again.

Once the 24-h solar irradiance curve has been determined, PV power output (P) can be calculated. Measurement studies presented in [20] indicate that P is linearly related with solar irradiance level. In addition, manufacturer's datasheets usually determine the peak power output of a PV cell when solar irradiance is 1000 W/m^2 [21], [22] and, therefore, it is assumed that the PV cell produces maximum power when Irr = 1000 W/m^2. Based on these characteristics, PV power output for a single snapshot may be mathematically estimated by (9), where min indicates the minimum of the two values within braces; Irr is the solar irradiance level in W/m^2, and $P_{\max}$ is the PV array maximum power output. Equation (9) is the default relationship to determine PV output power; the simulator was also developed to accept other user-defined relationships

$$P = \min \left\{ \frac{Irr}{1000 \ \text{W}/m^2} \times P_{\max}, P_{\max} \right\}. \tag{9}$$

This method may be adopted as a template for solar irradiance simulation on different locations. The parameter values presented in this paper (probability of occurrence of each CCL, cloud duration period, CCL correction factor, etc.) can be refined by using high-resolution measurement data if available for the location under study.

D. Deterministic Device Behavior

The capability to model deterministic events is also implemented in the proposed simulation platform. This feature is useful, for instance, for appliance identification. The user may wish to assign the exact time snapshot a certain appliance is switched-on in order to verify the effectiveness of its NILM algorithm. In addition, it may also be used to study energy storage control algorithms such as the ones discussed in [25], since its working cycle is deterministically related to house demand. A simple control technique consists on storing energy during power generation surplus, and providing energy during power generation shortage.

IV. NETWORK SOLUTION METHOD

There are 86 400 s over a 24 h period. Each second represent one snapshot of the network. For any particular snapshot,

the network configuration and the status of loads are known. This is a deterministic network scenario. Various power system solution techniques are developed to solve the scenario.

A. Fundamental Power Flow

The fundamental power flow calculation includes internal residential nodal voltages calculation in order to increase the simulator faithfulness to a real LV residential network. Both linear and nonlinear devices are modeled as constant power loads. Thus, an iterative method is selected to solve the nonlinear power flow equations. A two stage solution algorithm is adopted for each iteration, in order to reduce the network size and simplify the solution process at each step. Rated nodal voltages are used as an initial guess.

The first stage updates voltages outside the residence. In this stage, home loads are transformed into equivalent impedances using their current terminal voltage and correspondent power demand. With the obtained impedances, house equivalent admittance seen from service panel and network admittance matrix ($\mathbf{Y_N}$) can be readily calculated. Then, the matrix form of Kirchhoff's nodal law is solved to obtain an updated estimative of nodal voltages ($\mathbf{V'_N}$). $\mathbf{I_N}$ represents the nodal current injection. The nodal equation is shown in (10). In this process, PV arrays are simply regarded as negative constant power loads

$$\mathbf{Y_N}.\mathbf{V'_N} = \mathbf{I_N}. \tag{10}$$

The second stage updates voltages inside the residence. A new estimative for internal nodal voltages is determined, solving the circuit of Fig. 2 with load equivalent impedances and updated house service panel voltages ($\hat{V}'_{an}$, $\hat{V}'_{bn}$, $\hat{V}'_{ab}$).

After these two stages are performed, the difference (in per-unit) between the updated voltage ($\hat{V}'$) and the voltage of the previous iteration ($\hat{V}$) is determined for all network nodes. Then, the maximum voltage update is selected according to (11), where $V_{k-\text{rated}}$ is the rated voltage at node k and N is the number of nodes in the system. If $\Delta V(\%)$ is smaller than a threshold (e.g., 0.05%), the power flow solution has converged. Otherwise, the procedure must be repeated with updated nodal voltages ($\hat{V}'$)

$$\Delta V\,(\%) = 100 \times \frac{\max\left\{ \left|\hat{V}'_k - \hat{V}_k\right| \right\}}{V_{k-\text{rated}}} \quad k = 1, 2, \ldots, N. \tag{11}$$

This solution algorithm has been thoroughly tested on highly unbalanced networks. It has presented a robust convergence behavior (4–6 iterations) for all tested cases.

B. Harmonic Power Flow

Harmonic power flow results are needed to represent appliance signatures and to assess power quality impact. The solution algorithm adopted is also divided into the two stages as previously described, and uses information from the fundamental power flow solution. However, on harmonic frequencies, linear loads are modeled as impedances, and nonlinear loads as current sources. The current source magnitude and phase angle are calculated according to the typical harmonic current of the corresponding load. The current magnitude and phase angle are calculated according to (12), where the subscript spectrum refers to load typical harmonic current spectrum; $I_1 \angle \theta_1$ is the fundamental current injected from the load to the system and h is the harmonic order under study. The meaning of the magnitude formula is to scale up the typical harmonic current spectrum to match the fundamental frequency power flow result (I_1). The phase formula shifts the spectrum waveform to match the phase angle of θ_1. Since the hth harmonic has h-times higher frequency, its phase angle is shifted by h times of the fundamental frequency shift. Further details of this method are provided in [26]

$$I_h = I_1 \times \frac{I_{h-\text{spectrum}}}{I_{1-\text{spectrum}}}$$
$$\theta_h = \theta_{h-\text{spectrum}} + h \times \left(\theta_1 - \theta_{1-\text{spectrum}}\right). \tag{12}$$

Once all network parameters have been modeled either by impedance, or by current source, (10) may be solved for the frequency under study. As the network is modeled by impedances and current sources, the system solution becomes linear and no iteration is required.

C. Motor Starting Simulation

Traditional motors are still widely used in residential networks these days. Examples are dryer, furnace, and vacuum cleaner. The starting of such motors produces unique current spikes. These spikes have been found very useful for NILM algorithms as they represent motor loads. It is, therefore, important for the proposed platform to include motor starting transients.

A simplified induction motor dynamic behavior can be described as follows [27]:

$$J\frac{d\omega}{dt} = T_E - T_L \tag{13}$$

where J is motor inertia coefficient (kg.m^2); ω is rotor speed (rad/s); T_E is the electromagnetic torque produced by the motor (N.m); and T_L is the load torque applied to motor shaft (N.m).

Capacitor-start/capacitor-run single-phase induction motor is modeled, since it is generally used on single-phase motors [27]. The simulation algorithm can be described as follows.

Initially, default (or user input) values are assigned to motor parameters, such as impedances, inertia coefficient (J), rated slip (s_r), and rated efficiency (η_r). Then, one may calculate rated load torque according to (14), where ω_{sync} is the rotor synchronous speed in rad/s; and P_{in} is the power consumed by the motor in watts

$$T_{L-\text{rated}} = \frac{P_{out}}{\omega_{mec-\text{rated}}} = \frac{\eta_r \times P_{in}}{\omega_{\text{sync}} \times (1 - s_r)}. \tag{14}$$

Load torque relationship with rotor speed depends on load type. On fans (present in the furnace) torque depends on rotor speed squared, while on compressors (present in the fridge) load torque is constant for any rotor speed [28].
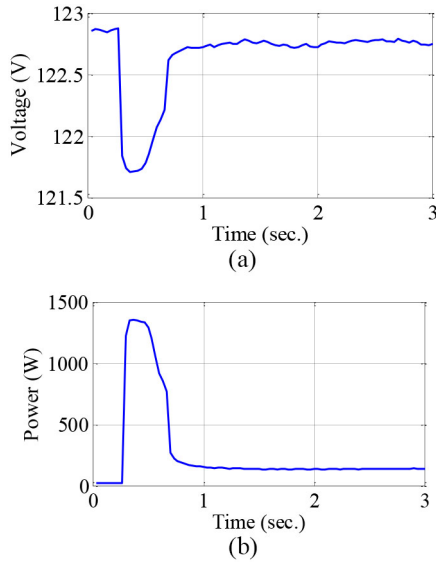
Fig. 7.   Measurement results during fridge starting transient. (a) Voltage sag. (b) Power spike.

Motor starting instant is randomly determined within a 1 s window, as in (15); where t_{cur} is the current simulation time, given in seconds

$$t = t_{cur} + \text{Unif}\left([0, \ 1]\right). \tag{15}$$

Once the motor starting instant has arrived, its speed $\omega(t + \Delta t)$ and correspondent slip $s(t + \Delta t)$ must be updated using (16), where Δt is the integration step and $T_E(t)$ is determined according to single-phase motor equivalent circuit for slip $s(t)$ (initial speed is zero and, consequently, initial slip is 1)

$$\omega\left(t + \Delta t\right) = \omega\left(t\right) + \frac{\Delta t}{J}\left[T_E\left(t\right) - T_L\left(t\right)\right]. \tag{16}$$

When (17) is satisfied, the motor equivalent power demand is calculated and one network power flow solution snapshot is performed using the algorithms described in Sections IV-A and B. This algorithm must be repeated for the next integration step $t + \Delta t$ until steady-state operation is achieved

$$t + \Delta t = n \times 1 \, \text{sec}, \quad n \text{ is integer.} \tag{17}$$

During the dynamic simulation process explained above, appliance terminal voltage is regarded as constant. Such assumption greatly simplifies the solution algorithm, since the terminal voltage does not need to be updated at every integration step Δt. It proves to be reasonable since real measurement data (Fig. 7) have shown that service panel voltage drop during motor start is around 0.01 p.u. and lasts for less than 1 s, while LV simulator resolution is 1 s. Fig. 8 presents a motor start simulation result.

D. Simulation of Multistage Appliances

Some appliances operate with multistage/multilevel demand characteristics. An example is the washing machine that has wash, rinse, and spinning modes. Modeling such appliances is essential for the simulator and is done as follows. Once an
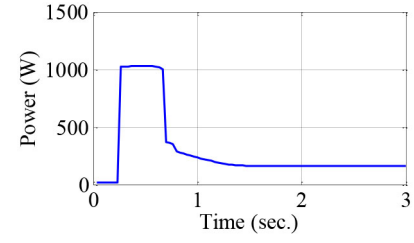

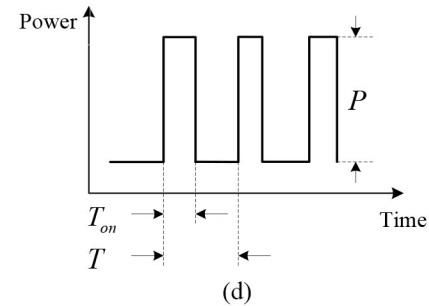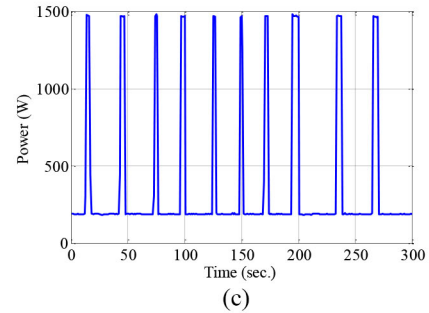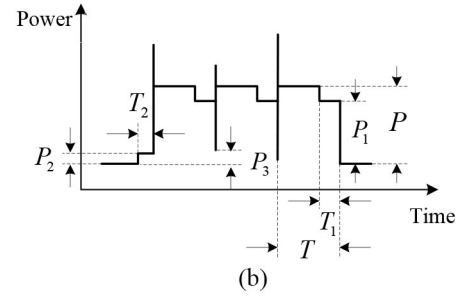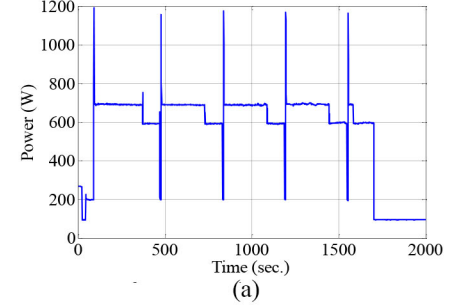Fig. 8.   Simulation results during a fridge starting transient.

Fig. 9.   Furnace and stove multistage and multilevel behavior. (a) Furnace-real measurement. (b) Furnace-simulation model. (c) Stove-real measurement. (d) Stove-simulation model.

appliance is ON, the simulator also models a set of random variables that compose its signature, as in Fig. 9. The furnace signature, for instance, has four power levels and three different stages [Fig. 9(a) and (b)]. The stove, on the other hand, is modeled only by one power level and two stages

TABLE II
FURNACE AND STOVE MULTILEVEL/MULTISTAGE MODEL

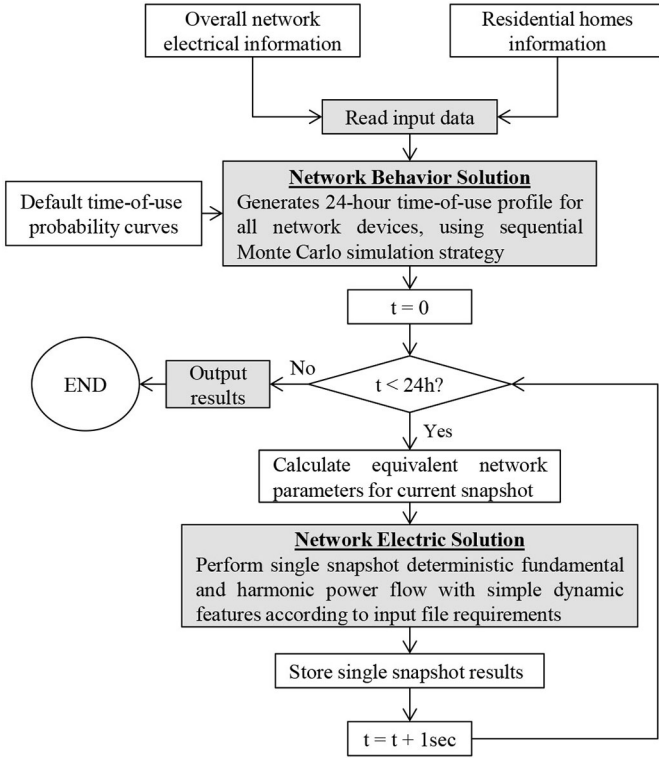| Furnace		Stove	
Variable	Value	Variable	Value
P	user-defined	P	user-defined
P_1/P	*Norm(0.8,0.01)*	T	*Norm(30s,2s)*
P_2/P	*Norm(0.2,0.01)*	T_{on}/T	*Unif([0.2,0.6])*
P_3/P	*Norm(0.2,0.001)*		
T	*Norm(360s,30s)*		
T_1/T	*Unif([0.3,0.7])*		
T_2	*60s*		

Fig. 10.   Overall LV network simulation platform flowchart.

[Fig. 9(c) and (d)]. A PDF is assigned to each of these variables according to typical measurement results, as shown in Table II. Finally, the furnace total working cycle duration is uniformly distributed within three and five sub-cycles of T seconds each, while the stove working cycle duration is uniformly distributed within 15 and 70 min. Other appliance models are not presented due to lack of space.

V. SUMMARY

The simulation tool proposed in this paper may be summarized with a high-level flowchart presented in Fig. 10, which is further described below.

An important goal considered during the platform design has been to develop it as an easy-to-use tool. Therefore, the "Read Input Data" routine provides a user-friendly input data structure divided into two files, which are described as follows.

1) *Network Electrical Information:* This file contains utility related information (primary network equivalent, transformer parameters, distribution lines parameters, grounding impedances, etc.), in addition to nonlinear appliances harmonic spectrum. Default information is provided for all parameters, for the user unfamiliar with such electrical data.

2) *Residential Homes Information:* This file contains household device connections. The user must specify which devices are installed at which room. A generic type and number of appliances can be specified, which provides the user with great flexibility to create a realistic house scenario. The only electrical information required is the device rated power and power factor. Therefore, this file may be edited by any user, even those not familiar with network electrical concepts. Additionally, specific non-default appliance behavior patterns can also be provided on this input file.

The input information feeds the "network behavior solution" core, which determines all household devices states throughout the simulation. If no specific behavior information is provided by the user for a device, default time-of-use probability curves are considered. Then, for each time snapshot, corresponding device states are retrieved, equivalent network parameters are calculated, and the "network electric solution" core is executed. After each electric solution snapshot, fundamental and harmonic voltages at house service panel are stored. Then, based on house equivalent impedances, both power and current demand at each phase are determined. Once the simulation has finished, "output results" routine is performed to provide the study outcome in a table format with the output variables behavior over the simulated period. Results may be later read and processed according to user needs.

A prototype platform has been developed using MATLAB environment. In terms of computational load, the highest efforts involved are the calculation and factorization of the network admittance matrices at the fundamental and harmonic frequencies. The simulation time of 1 snapshot on a 10-house network with over 100 appliances (about 250 nodes) up to the ninth harmonic is approximately 100 ms on a standard PC. This computing speed can be drastically reduced if sparse matrix techniques, code optimization, and C-based programming language are used.

Fig. 11 shows an example power demand and third harmonic profile of a home produced by the simulator over a 24 h period.

VI. CASE STUDIES

This section presents several case study results. They are used to illustrate the potential applications of the platform.

A. Home Appliance Identification

The first case study consists on evaluating the effectiveness of the NILM algorithm proposed in [3]. A 5-day simulation is performed using the platform. The power demand profile for one household over the 5 days is fed into the appliance identification program. The success rate of appliance identification for some of the major appliances is shown in Table III.

B. PV Array Integration Impacts

A utility company may want to investigate technical impacts arisen from the increasing connection of residential rooftop
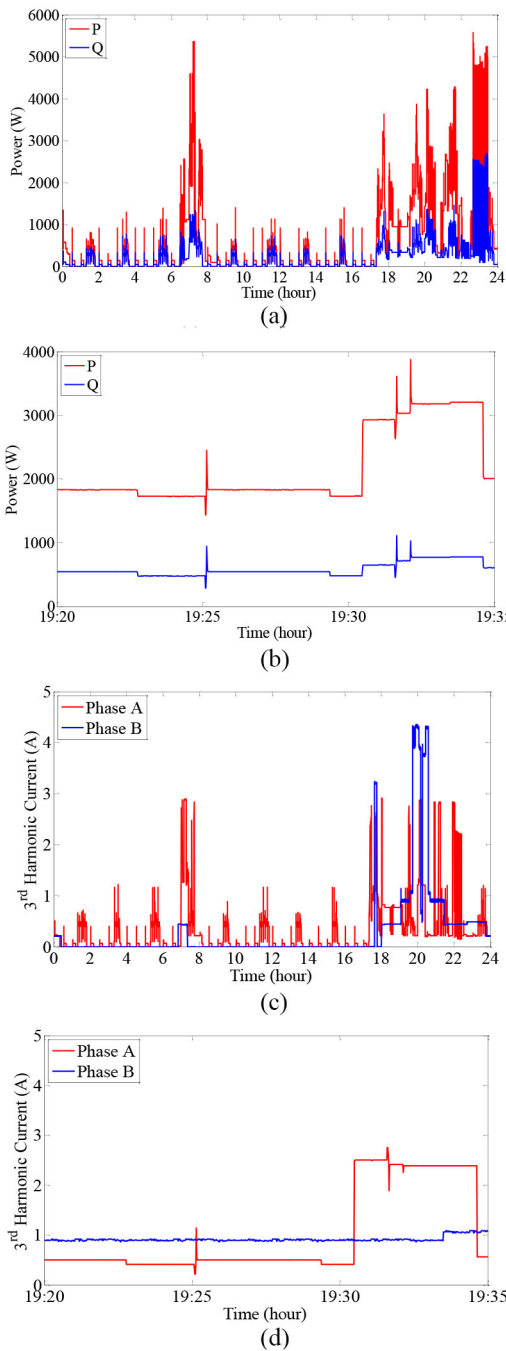
Fig. 11. Sample power demand and third harmonic simulation results. (a) 24-h profile. (b) 15-min detailed profile. (c) 24-h profile. (d) 15-min detailed profile.

PV arrays on LV networks. To achieve such goal, a sample case study is performed on a 10-house network scenario. On the considered network, five houses are randomly selected to contain PV arrays with ratings within 2–3 kWp. The PV arrays are phase-to-phase connected to avoid system unbalance. A clear day is considered. Fig. 12 compares the 1-min average service panel phase voltages before and after PV integration. Simulation results can identify a voltage rise around noon, since this is the time with maximum PV power output during the day, due to maximum solar irradiance. Such results outline that overvoltages during the day may become a concern for the utility according to PV consumer adoption levels.

TABLE III
SUCCESS RATE OF APPLIANCE IDENTIFICATION

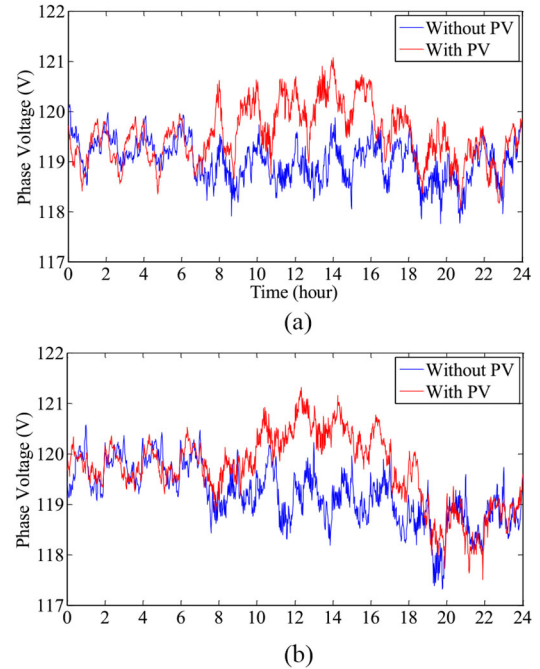| Appliance name	Identified / Actual operation times	Appliance name	Identified / Actual operation times
Fridge	218 / 240	Dryer	2 / 2
Freezer	345 / 360	Laptop	3 / 3
Microwave	31 / 36	PC + monitor	3 / 4
Stove	14 / 14	LCD TV	9 / 9
Furnace	56 / 60	CFL	14 / 17
Washer	2 / 2	Toaster	4 / 4

Fig. 12. PV array integration impact on service panel voltages. (a) Phase A. (b) Phase B.

TABLE IV
95%-INDEX OF NEV FOR DIFFERENT NEUTRAL CONDITIONS

Normal neutral	Damaged neutral	Difference
1.08 V	1.83 V	69.4%

The simulation platform is also suitable for more detailed studies, such as to identify the impacts of an increasing PV penetration trend over the years.

C. Impact of Neutral Condition on NEV

In this example, the impact of neutral condition on NEV at the service entrance point of a home is investigated. NEV has been considered as the main source of stray voltage at residential homes [7]. To simulate a damaged neutral condition, an impedance of 0.3Ω is added in series with the neutral conductor connected to one of the ten houses on the network. According to Table IV and Fig. 13, a damaged neutral condition will negatively impact the NEV, increasing the risk of stray voltage incidents. The 95%-index presented in Table IV indicates the NEV values that are not exceeded during 95% of the simulation duration (24 h).
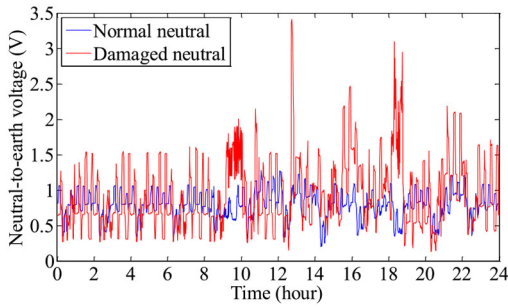
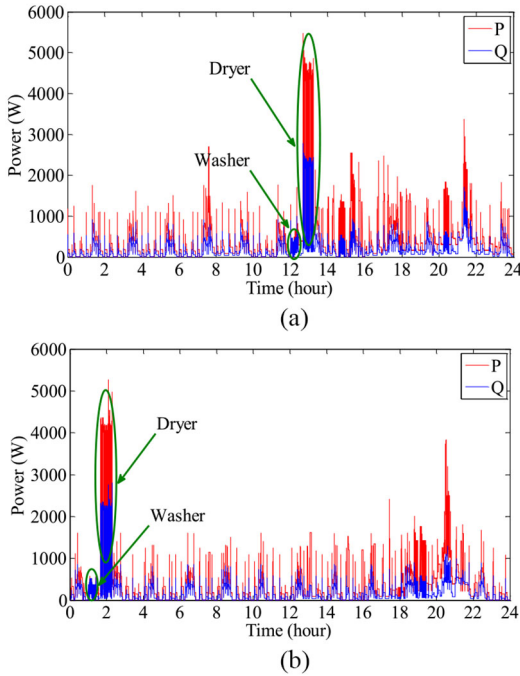Fig. 13. Impact of neutral condition on neutral-to-earth voltage level.

Fig. 14. Demand response technique evaluation on LV simulator. (a) Before appliance shifting. (b) After appliance shifting.

TABLE V
DAILY EXPENSE SAVING WITH DEMAND RESPONSE STRATEGY APPLICATION

	Energy demand (kWh)	Total expense (CAD ¢)
Before appliance shifting	8.02	79.2
After appliance shifting	8.03	68.4

D. Demand Response Analysis

In this example, the proposed platform is used to evaluate a demand response strategy. It consists on scheduling the laundry activity (washer and dryer working cycles), which is more likely to occur from 8:00 to 15:00 (Fig. 4), to an off peak time, in order to take advantage of a time dependent tariff. The proposed demand response strategy is evaluated on the simulation tool and the result is presented in Fig. 14.

The strategy effectiveness is confirmed by over 10% electricity bill reduction (Table V). Ontario, Canada time dependent tariff [29] was considered in this paper.

VII. CONCLUSION

An SMC simulation platform for residential networks has been proposed. This platform can be used to assist the research and development of various demand-side based smart-grid techniques. It can also be used to verify and demonstrate such techniques. The platform consists of two main components. The first is a multiphase network model with power flow, harmonic and motor starting study capabilities. The second is a load/generation behavior model that established the operating characteristics of various loads/generators based on time-of-use probability curves. These two components are combined together through an SMC simulation scheme. The usefulness of the platform has been demonstrated through application case studies. The proposed tool can be expanded by including more loads or generators and by simulating additional electrical responses of the network such as flicker and vehicle to grid operation.

REFERENCES

[1] K. Hamilton and N. Gulhar, "Taking demand response to the next level," *IEEE Power Energy Mag.*, vol. 8, no. 3, pp. 60–65, May/Jun. 2010.

[2] G. W. Hart, "Nonintrusive appliance load monitoring," *Proc. IEEE*, vol. 80, no. 12, pp. 1870–1891, Dec. 1992.

[3] M. Dong, P. C. M. Meira, W. Xu, and W. Freitas, "An event window based load monitoring technique for smart meters," *IEEE Trans. Smart Grid*, vol. 3, no. 2, pp. 787–796, Jun. 2012.

[4] Y. Chen, C. Chu, S. Tsao, and T. Tsai, "Detecting users' behaviors based on nonintrusive load monitoring technologies," presented at the 10th IEEE Int. Conf. Netw., Sensing Control (ICNSC), Evry, France, 2013.

[5] J. Liang, S. Ng, G. Kendall, and J. Cheng, "Load signature study—Part I: Basic concept, structure, and methodology," *IEEE Trans. Power Del.*, vol. 25, no. 2, pp. 551–560, Apr. 2010.

[6] D. Srinivasan, W. S. Ng, and A. C. Liew, "Neural-network-based signature recognition for harmonic source identification," *IEEE Trans. Power Del.*, vol. 21, no. 1, pp. 398–405, Jan. 2006.

[7] J. Burke and C. Untiedt, "Stray voltage: Two different perspectives," *IEEE Ind. Appl. Mag.*, vol. 15, no. 3, pp. 36–41, May/Jun. 2009.

[8] M. Pipattanasomporn, M. Kuzlu, and S. Rahman, "An algorithm for intelligent home energy management and demand response analysis," *IEEE Trans. Smart Grid*, vol. 3, no. 4, pp. 2166–2173, Dec. 2012.

[9] R. Garcia-Valle, L. C. P. da Silva, Z. Xu, and J. Ostergaard, "Smart demand for improving short-term voltage control on distribution networks," *IET Gen. Transmiss. Distrib.*, vol. 3, no. 8, pp. 724–732, Aug. 2009.

[10] "Operator training simulator," Elect. Power Res. Inst., Palo Alto, CA, USA, Tech. Rep. EL-7244, May 1991.

[11] A. Doucet, N. de Freitas, and N. Gordon, Eds., *Sequential Monte Carlo Methods in Practice*. New York, NY, USA: Springer, 2001.

[12] A. Doucet, S. Godsill, and C. Andrieu, "On sequential Monte Carlo sampling methods for Bayesian filtering," *Statist. Comput.*, vol. 10, no. 3, pp. 197–208, 2000.

[13] R. Hendron, "Building America research benchmark definition," Dept. Energy Office Energy Efficiency Renewable Energy, Nat. Renewable Energy Lab., Golden, CO, USA, Tech. Rep. NREL/TP-550-40968, 2007.

[14] IPSOS-RSL and Office for National Statistics, *United Kingdom Time Use Survey, 2000*, 3rd ed. Colchester, U.K., U.K. Data Archive, 2003.

[15] K. Qian, C. Zhou, M. Allan, and Y. Yuan, "Modeling of load demand due to EV battery charging in distribution systems," *IEEE Trans. Power Syst.*, vol. 26, no. 2, pp. 802–810, May 2011.

[16] J. A. Orr, A. E. Emanuel, and D. G. Pileggi, "Current harmonics, voltage distortion, and powers associated with battery chargers—Part I: Comparisons among different types of chargers," *IEEE Trans. Power App. Syst.*, vol. PAS-101, no. 8, pp. 2703–2710, Aug. 1982.

[17] G. S. Campbell and J. M. Norman, *An Introduction to Environmental Biophysics*, vol. 1, 2nd ed. New York, NY, USA: Springer, 2000, pp. 173–175.

IEEE TRANSACTIONS ON SMART GRID, VOL. 5, NO. 6, NOVEMBER 2014

[18] S. A. Arefifar, Y. A. I. Mohamed, and T. H. M. El-Fouly, "Supply-adequacy-based optimal construction of microgrids in smart distribution systems," *IEEE Trans. Smart Grid*, vol. 3, no. 3, pp. 1491–1502, Sep. 2012.

[19] (Jun. 2014). *Edmonton Clear Sky Chart History* [Online]. Available: http://cleardarksky.com/clmt/c/Edmontonct.html

[20] G. TamizhMani, K. Paghasian, J. Kuitche, M. G. Vemula, and G. Sivasubramanian. (2011). "Photovoltaic module power rating per IEC 61853-1 standard: A study under natural sunlight," Solar America Board for Codes and Standards, Mesa, AZ, USA [Online]. Available: http://www.solarabcs.org/about/publications/reports/pv-mod-power-rating/pdfs/PVModulePowerRatingReport.pdf

[21] Sunpower. (Jun. 2014). *E20/435 Solar Panel, Datasheet* [Online]. Available: http://www.solarplaza.com/top10-monocrystalline-cell-efficiency/#Suntech

[22] Sanyo, *HIT Photovoltaic Modules, Datasheet* [Online]. Available: http://www.solarplaza.com/top10-monocrystalline-cell-efficiency/#Suntech

[23] (Jun. 2014). *Current and Historical Alberta Weather Station Data Viewer, Alberta Agriculture and Rural Development* [Online]. Available: http://www.agric.gov.ab.ca/acis/alberta-weather-data-viewer.jsp

[24] J. Kleissl. (Jun. 2014). *Current State of the Art in Solar Forecasting.* California Institute for Energy and Environment [Online]. Available: http://uc-ciee.org/downloads/appendixA.pdf

[25] S. Teleke, M. E. Baran, S. Bhattacharya, and A. Q. Huang, "Rule-based control of battery energy storage for dispatching intermittent renewable sources," *IEEE Trans. Sustain. Energy*, vol. 1, no. 3, pp. 117–124, Oct. 2010.

[26] Task force on harmonics modeling and simulation, "Modeling and simulation of the propagation of harmonics in electric power networks—Part I: Concepts, models, and simulation techniques," *IEEE Trans. Power Del.*, vol. 11, no. 1, pp. 452–465, Jan. 1996.

[27] P. C. Sen, *Principles of Electric Machines and Power Electronics*, vol. 1, 2nd ed. Hoboken, NJ, USA: Wiley, 1997.

[28] A. K. Wallace, R. Spée, and L. G. Martin, "Current harmonics and acoustic noise in AC adjustable-speed drives," *IEEE Trans. Ind. Appl.*, vol. 26, no. 2, pp. 267–273, Mar./Apr. 1990.

[29] IESO (2013, Jun.). *Time-Of-Use Prices*. [Online]. Available: http://www.ieso.ca/imoweb/siteshared/tou_rates.asp?sid=ic

Ricardo Torquato (S'11) is currently pursuing the M.Sc. degree in electrical engineering from the University of Campinas, Campinas, Brazil.

He is currently a Visiting Student with the University of Alberta, Edmonton, AB, Canada. His research interests include power quality and analysis of distribution systems.

Qingxin Shi (S'11) is currently pursuing the M.Sc. degree in electrical engineering from the University of Alberta, Edmonton, AB, Canada.

His research interests include power quality and power signaling.

Wilsun Xu (M'90–SM'95–F'05) received the Ph.D. degree in electrical engineering from the University of British Columbia, Vancouver, BC, Canada, in 1989.

He is currently a Professor and a Natural Sciences and Engineering Research Council of Canada/Informatics Circle of Research Excellence (NSERC/iCORE) of Alberta Industrial Research Chair with the University of Alberta, Edmonton, AB, Canada. His research interests include power quality and information extraction from power disturbances.

Walmir Freitas (M'02) received the Ph.D. degree in electrical engineering from the University of Campinas, Campinas, Brazil, in 2001.

He is currently an Associate Professor with the University of Campinas. His research interests include distribution systems, power quality, and distributed generation.